The 2022 World Congress on
The 2022 Structures Congress (Structures22)
16-19, August, 2022, GECE, Seoul, Korea

The MITC4+ shell finite element with a simplified assumed membrane strain field

Hyung-Gyu Choi[1)] and *Phill-Seung Lee[2)]

[1), 2)] *Department of Mechanical Engineering, KAIST, Daejeon 305-600, Korea*
[2)] *phillseung@kaist.edu*

ABSTRACT

When the geometry of the original MITC4 element is distorted, the performance of the element deteriorates with revealing membrane locking phenomenon. The recently developed MITC4+ shell element successfully alleviates the membrane locking by assuming the locking-causing term with linear combination of sampled strains. However, one drawback of the MITC4+ element is that its formulation is quite complex to implement. In this study, the MITC4+ shell finite element with a simplified assumed membrane strain field is presented. The proposed element passes all the basic tests including patch, zero energy mode and isotropy tests. In widely-used shell benchmark problems, the convergence behavior of the proposed element is studied and compared with the MITC4+ shell element.

1. INTRODUCTION

For decades, the analysis of shell structures has been mainly performed using the finite element method. There are various types of shell finite elements, but among them, elements based on the mixed interpolation of tensorial components (MITC) method are frequently used (Bathe 2003, Lee 2007, Ko 2017, Lee 2022). The MITC method was first proposed to alleviate transverse shear locking at the 4-node quadrilateral shell element (MITC4) (Dvorkin 1984). The MITC4 element shows excellent convergence behavior in uniform meshes (Joen 2014). However, the performance of the MITC4 element substantially deteriorates with revealing membrane locking phenomenon when the geometry of the element is distorted in bending dominated shell problems (Ko 2016).

Recently, the MITC4+ element has been developed by Ko et al. The MITC4+ element successfully alleviates the membrane locking by assuming the locking-causing term with linear combination of sampled strains. The MITC4+ element shows almost

[1)] Graduate Student
[2)] Professor

optimal convergence behavior in various shell benchmark problems. However, one drawback of the MITC4+ element is that its formulation is quite complex to implement.

In this study, we focus on simplifying the formulation of the MITC4+ element. The complicated assumed membrane strain field is replaced by a simplified assumed membrane strain field and consequently a new MITC4+ element is developed. The new MITC4+ element passes all the basic tests including patch, zero energy mode and isotropy test and shows slightly better performance than that of the MITC4 element.

In the following sections, the formulation of the new MITC4+ element is briefly presented. We also demonstrated the performance of the new MITC4+ element through shell benchmark problems.

2. ASSUMED MEMBRANE STRAIN FIELD

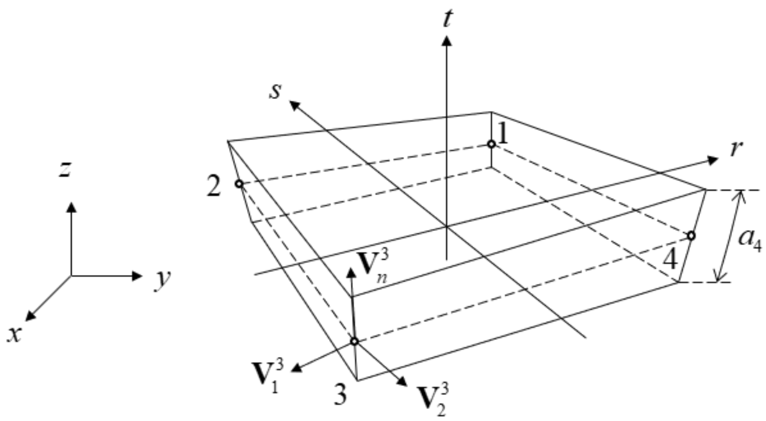

Fig. 1 A 4-node quadrilateral shell finite element.

As shown in Fig. 1, the geometry and displacement of the 4-node quadrilateral shell element are interpolated as (Ko 2017).

$$\mathbf{x} = \sum_{i=1}^{4} h_i(r,s)\mathbf{x}_i + \frac{t}{2}\sum_{i=1}^{4} a_i h_i(r,s)\mathbf{V}_n^i \quad \text{with} \quad \mathbf{x}_i = \begin{bmatrix} x_i & y_i & w_i \end{bmatrix}^{\mathrm{T}}, \tag{1}$$

$$\mathbf{u} = \sum_{i=1}^{4} h_i(r,s)\mathbf{u}_i + \frac{t}{2}\sum_{i=1}^{4} a_i h_i(r,s)(-\alpha_i \mathbf{V}_2^i + \beta \mathbf{V}_1^i) \quad \text{with} \quad \mathbf{u}_i = \begin{bmatrix} u_i & v_i & w_i & \alpha_i & \beta_i \end{bmatrix}^{\mathrm{T}}, \tag{2}$$

where $\mathbf{x}_i$ and $\mathbf{u}_i$ are the nodal position and displacement vectors, respectively, a_i is the nodal thickness, and h_i is the shape function which is given by (Lee 2018, 2021)

$$h_1 = \frac{1}{4}(1+r)(1+s), \quad h_2 = \frac{1}{4}(1-r)(1+s), \quad h_3 = \frac{1}{4}(1-r)(1-s), \quad h_4 = \frac{1}{4}(1+r)(1-s). \tag{3}$$

We here briefly introduce a simplified assumed membrane strain field for a new MITC4+ element. The covariant in-plane strain components are given as

$$e_{ij} = e_{ij}^{m} + te_{ij}^{b1} + t^2 e_{ij}^{b2} \quad \text{with} \quad i, j = 1,2, \tag{4}$$

where e_{ij}^{m} is the covariant membrane strain and the remaining terms including e_{ij}^{b1} and e_{ij}^{b2} denote the covariant bending strain. The strain decomposition into the membrane, bending, and transverse shear strains is well described in Ko et al (Ko 2017).

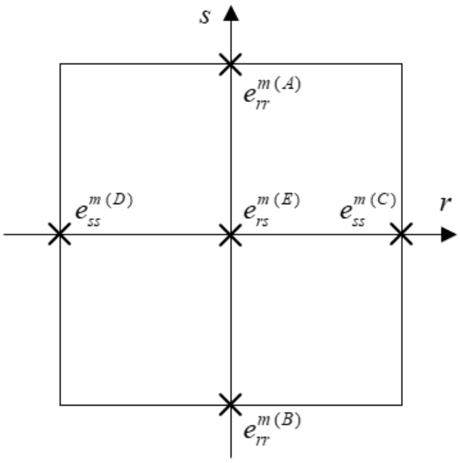

Fig. 2 Tying points (A)-(E) for the MITC4+ element.

To alleviate the membrane locking in the MITC4+ element, the covariant membrane strain field is assumed using five tying points (A)-(E) as shown in Fig. 2,

$$\begin{aligned}\hat{e}_{rr}^{m} &= \frac{1}{2}(1-2a_A + s + 2a_A \cdot s^2)e_{rr}^{m(A)} + \frac{1}{2}(1-2a_B - s + 2a_B \cdot s^2)e_{rr}^{m(B)} \\ &\quad + a_C(-1+s^2)e_{ss}^{m(C)} + a_D(-1+s^2)e_{ss}^{m(D)} + a_E(-1+s^2)e_{rs}^{m(E)}\end{aligned} \tag{5}$$

$$\begin{aligned}\hat{e}_{ss}^{m} &= a_A(-1+r^2)e_{rr}^{m(A)} + a_B(-1+r^2)e_{rr}^{m(B)} + a_E(-1+r^2)e_{rs}^{m(E)} \\ &\quad + \frac{1}{2}(1-2a_C + r + 2a_C \cdot r^2)e_{ss}^{m(C)} + \frac{1}{2}(1-2a_D - r + 2a_D \cdot r^2)e_{ss}^{m(D)}\end{aligned} \tag{6}$$

$$\begin{aligned}\hat{e}_{rs}^{m} &= \frac{1}{4}(r + 4a_A \cdot rs)e_{rr}^{m(A)} + \frac{1}{4}(-r + 4a_B \cdot rs)e_{rr}^{m(B)} + \frac{1}{4}(s + 4a_C \cdot rs)e_{ss}^{m(C)} \\ &\quad + \frac{1}{4}(-s + 4a_D \cdot rs)e_{ss}^{m(D)} + (1 + a_E \cdot rs)e_{rs}^{m(E)}\end{aligned} \tag{7}$$

$$a_A = \frac{c_r(c_r-1)}{2d},\ a_B = \frac{c_r(c_r+1)}{2d},\ a_C = \frac{c_s(c_s-1)}{2d},\ a_D = \frac{c_s(c_s+1)}{2d},\ a_E = \frac{2c_r c_s}{d} \tag{8}$$

In the formulation of the new MITC4+ element, the membrane strain components are expressed by using constant base vectors as

$$\mathbf{e}^m = \hat{e}^m_{ij}(\hat{\mathbf{g}}^i \otimes \hat{\mathbf{g}}^j) \ \text{ with } \ i,j=1,2, \tag{9}$$

in which $\hat{\mathbf{g}}^i$ is the contravariant base vector evaluated at the element center ($r=s=0$).

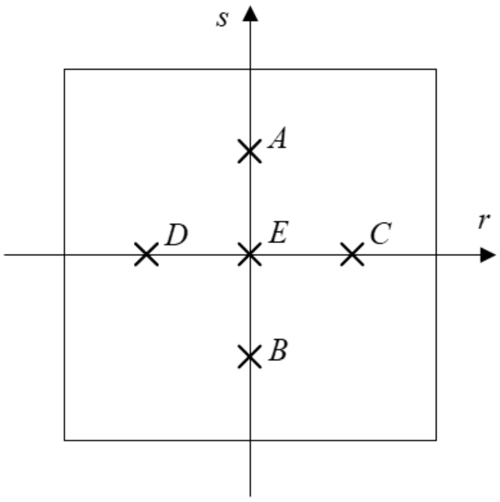

Fig. 3 Tying points (A)-(E) for the new MITC4+ element.

Then, the simplified assumed membrane strain field is constructed using the tying points (A)-(E) as shown in Fig. 3.

$$\tilde{e}^m_{rr} = \hat{e}^{(E)}_{rr} + \frac{1}{2l}\lambda(r,s)\left(\hat{e}^{(A)}_{rr} - \hat{e}^{(B)}_{rr}\right)s, \tag{10}$$

$$\tilde{e}^m_{ss} = \hat{e}^{(E)}_{ss} + \frac{1}{2l}\lambda(r,s)\left(\hat{e}^{(C)}_{ss} - \hat{e}^{(D)}_{ss}\right)r, \tag{11}$$

$$\tilde{e}^m_{rs} = \hat{e}^{(E)}_{rs}, \tag{12}$$

where l is the distance between tying points (A)-(D) and the element center, and λ is the ratio of the determinants of the Jacobian matrices. The simplified assumed membrane strain field is obtained by taking the distance close to the element center.

For the treatment of the transverse shear locking in both the MITC4+ and new MITC4+ elements, the well-known assumed transverse shear strain field of the MITC4 element is adopted (Dvorkin 1984).

3. Numerical example

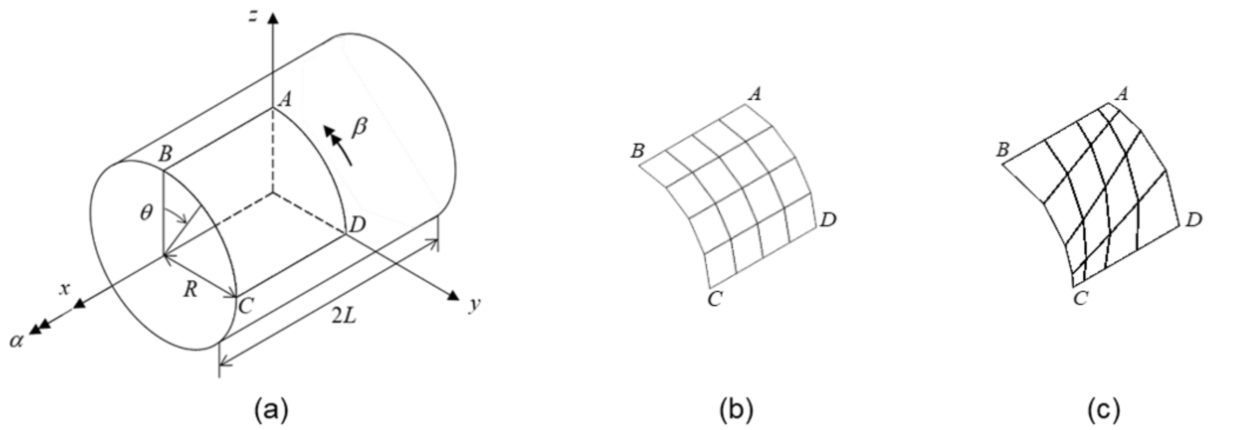

Fig. 4 (a) Cylindrical shell problem ($L = R = 1$, $E = 2.0\times10^5$, and $\nu = 1/3$). (b) Regular mesh when $N = 4$. (C) Distorted mesh when $N = 4$.

In this section, the convergence behavior of the new MITC4+ is studied and compared with the MITC4 and MITC4+ shell elements. As shown in **Fig. 4**, the cylindrical shell with free ends is considered for the bending dominated problem (Ko 2017, Lee 2019). The length is $2L$, the radius is R, and the thickness is t. The structure is subjected to a varying pressure $p(\theta) = \cos(2\theta)$. The regular and distorted meshes are depicted in **Figs. 4(b)** and **4(c)**, respectively. Based on the symmetry of the problem, only one-eighth of the shell structure is modeled. For the boundary conditions, $u_y = \alpha = 0$ along AB, $u_x = \beta = 0$ along AD, and $u_z = \alpha = 0$ along CD.

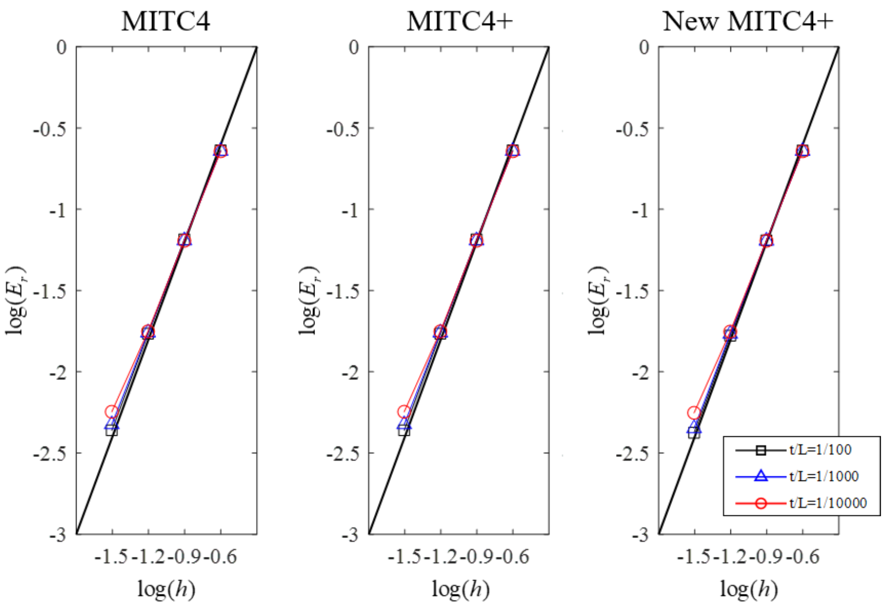

Fig. 5 Convergence curves for the free cylindrical shell problem with regular meshes

Solutions for both regular and distorted meshes are obtained with $N \times N$ meshes (N=4, 8, 16, and 32). The relative error is evaluated using the reference strain energy obtained by a 64×64 mesh of MITC9 shell elements. Figs. 5 and 6 show the convergence curves for the free cylindrical shell problem with the regular and distorted meshes, respectively. The element size in the convergence curves is denoted as $h = L / N$. When the regular meshes are used, all shell elements considered perform well. However, for the distorted mesh case, the MITC4+ and new MITC4+ elements show much better predictive capability than that of the MITC4 element.

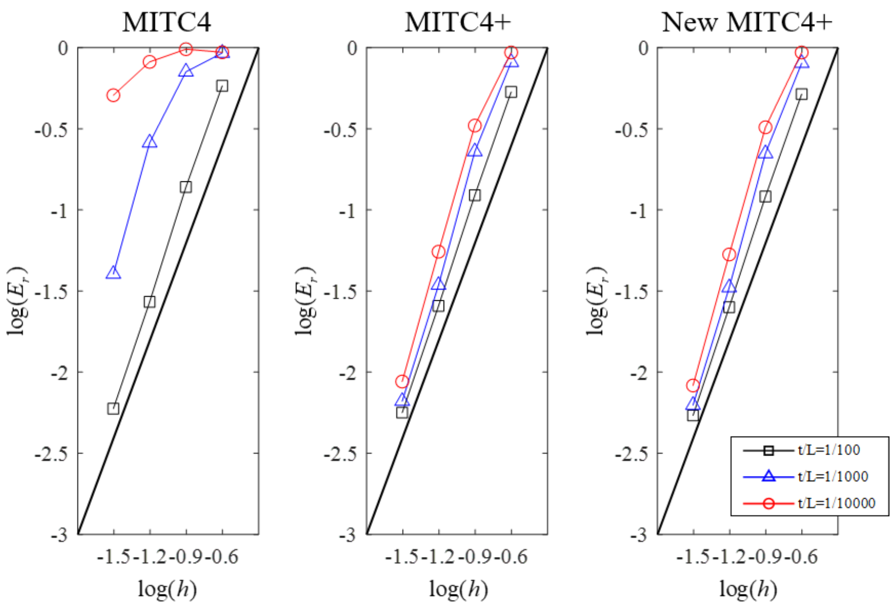

Fig. 6 Convergence curves for the free cylindrical shell problem with distorted meshes

4. CONCLUSIONS

In this study, the simplified assumed membrane strain field is introduced for the MITC4+ shell finite element while keeping its excellent performance. The new MITC4+ element passes the isotropy, patch and zero energy mode tests. Through numerical example, the convergence behavior of the element is studied and compared with the MITC4 and MITC4+ elements. In future work, the proposed element can be extended for solving non-linear problems.

ACKNOWLEDGEMENTS

This work was supported by the National Research Foundation of Korea (NRF) grant funded by the Korea government (MSIT) (No. NRF-2018R1A2B3005328).

REFERENCES

Dvorkin, E.N., Bathe, K.J. (1984), A continuum mechanics based four node shell element for general non-linear analysis, Engineering Computations, 1, 77-88.

Bathe, K.J., Lee, P.S., Hiller, J.F. (2003), Towards improving the MITC9 shell element, Computers and Structures, 81(8-11), 477-489.

Lee, P.S., Noh, H.C., Bathe, K.J. (2007). Insight into 3-node triangular shell finite elements: the effects of element isotropy and mesh patterns, Computers and Structures, 85(7-8), 404-418.

Ko, Y., Lee, P.S., Bathe, K.J. (2017), A new 4-node MITC element for analysis of two-dimensional solids and its formulation in a shell element, Computers & Structures, 192, 34-49.

Lee, C., Lee, D.H., Lee, P.S. (2022), The strain-smoothed MITC3+ shell element in nonlinear analysis, Computers & Structures, 265, 106768.

Ko, Y., Lee, P.S., Bathe, K.J. (2017), A new MITC4+ shell element, Computers & Structures, 182, 404-418.

Lee C, Lee PS. (2018), A new strain smoothing method for triangular and tetrahedral finite elements. Comput Methods Appl Mech Eng 2018;341:939–55.

Ko, Y., Lee, Y., Lee, P.S., Bathe, K.J. (2017), Performance of the MITC3+ and MITC4+ shell elements in widely-used benchmark problems, Computers & Structures, 193, 187-206.

Lee, C., Lee, P.S. (2019), The strain-smoothed MITC3+ shell finite element, Computers & Structures, 223, 106096.

Ko, Y., Lee, P.S., Bathe, K.J. (2017), The MITC4+ shell element in geometric nonlinear analysis, Computers & Structures, 185, 1-14.

Lee C, Kim S, Lee PS. (2021), The strain-smoothed 4-node quadrilateral finite element. Comput Methods Appl Mech Eng 2021;373:113481.

Jeon HM, Lee PS, Bathe KJ. (2014), The MITC3 shell finite element enriched by interpolation covers. Comput Struct 2014;134:128–42.